04-83-10.

Journal of Nuclear Materials 119 (1983) 59–66
North-Holland, Amsterdam

^{51}Cr DIFFUSION IN α-Zr SINGLE CRYSTALS

S.N. BALART [1], N. VARELA [2] and R.H. de TENDLER [1]

[1] *Departamento de Materiales, Comisión Nacional de Energía Atómica, Av. del Libertador 8250, 1429 Buenos Aires, Argentina*
[2] *Centro de Investigaciones Textiles, Instituto Nacional de Tecnologia Industrial, Av. Gral. Paz e/Albarellos y Constituyentes, 1650 San Martin, Pcia. de Buenos Aires, Argentina*

Received 27 May 1983; accepted 8 June 1983

The volume diffusion coefficients of the fast-diffusing solute ^{51}Cr have been obtained in oriented α-Zr single crystals, in the directions parallel and perpendicular to the *c* axis. The dependence of these diffusion coefficients on temperature was also measured between 750°C and 848°C.

Single crystals were grown by thermal cycling through the $\alpha \leftrightarrow \beta$ transformation temperature (862°C). Diffusion coefficients were measured using the "thin film" method. In some experiments non-Gaussian penetration profiles were obtained and this behaviour is also analyzed.

The diffusion of ^{51}Cr is faster in the *c* axis direction, with $Q_{\parallel}$(153 kJ/mol) < $Q_{\perp}$(163 kJ/mol). The anisotropy factor $f_a = D_{\parallel}/D_{\perp} \approx 3$. This factor, the activation energies and frequency factors are discussed in comparison with those of other solutes.

1. Introduction

α-Zr belongs to a class of solvents which admit extremely fast-diffusing solutes [1,2]. Volume diffusivities of Co [3], Ni [4], Fe [1,4,5], Be [6], Cu [7], Cr [8] and Mn [9] in α-Zr have been determined by different authors, and show values which are 3 to 7 orders of magnitude * larger than self-diffusion. To explain this behaviour, a model has been considered for the heterodiffusion mechanism in which one additional non-substitutional state is available for the solute. This state is responsible for the fast diffusion and is closely related to the interstitial configuration [1,2].

Because α-Zr is anisotropic, differences in the value of the diffusivity along the *c* axis or perpendicular to it might be expected in self- and in heterodiffusion.

In studies of ^{51}Cr diffusion in coarse-grained polycrystals of Zr–Sn alloys [11], a remarkable contrast was found between the small but quite definite effect of the Sn concentration on ^{51}Cr diffusivity in the β-phase and the lack of a similarly clear correlation in the α-phase. In the three experiments performed in the α-phase, the ^{51}Cr diffusivity in polycrystals of pure α-Zr was also measured. These values showed an appreciable scatter with respect to the previously determined Arrhenius plot for ^{51}Cr diffusion in polycrystalline α-Zr [8].

Both results could be ascribed to the anisotropy of the α-phase and the presence of variously oriented grains in different samples [12], an explanation that motivated the present work.

Our aim was to reveal and quantify this anisotropy through measurements of ^{51}Cr diffusion coefficients in α-Zr single crystals in the directions parallel and perpendicular to the *c* axis. The dependence of these diffusion coefficients on temperature was determined between 750°C and 848°C.

* This range of values can be 3 to 7 [1] or 5 to 9 [3] depending on which value for self-diffusion is adopted: that for polycrystals [10] or the one value measured in single crystals found in the literature [5].

2. Experimental

2.1. Growth of α-Zr single crystals

The single crystals of α-Zr used in this study were grown by thermal cycling through the $\alpha \leftrightarrow \beta$ transformation temperature [13].

Cylindrical samples 1.27 cm in diameter and 0.6–0.8 cm thick were cut from as-received rods of Zr 99.99% purity (Zr I) and subjected to the thermal cycling shown schematically in fig. 1.

0022-3115/83/$03.00

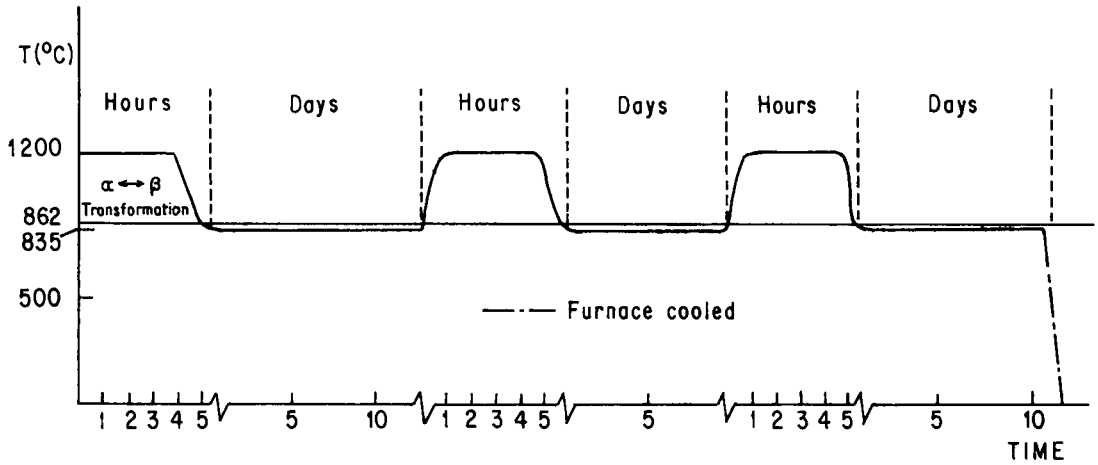

Fig. 1. Scheme of the thermal-cycle applied to grow α-Zr single crystals.

Before annealing, the samples were mechanically polished and subjected to electrolytic polishing in a cooled solution of butyl-cellosolve and perchloric acid 90 : 10, and cleaned with boiling ethyl ether.

Anneals were performed in an Ar atmosphere. The samples, enclosed in Ta cylinders, were placed inside a quartz tube which was evacuated to 10^{-7} Torr, pre-heated and sealed after introducing Ar (99.998% pure). The arrangements during the anneals were much the same as those employed in the diffusion anneals.

This method provided single to tetra-crystals from which individual grains were extracted by spark-cutting. The size of these crystals ranged from 0.45 cm to 1.27 cm in diameter and 0.6 cm to 0.8 cm thick. They had a well stabilized structure due to the last long anneal in the α-phase (fig. 1). Their quality was confirmed by the sharpness of the spots in Laue back-reflection X-rays diagrams. The unit stereographic triangle in fig. 2 shows

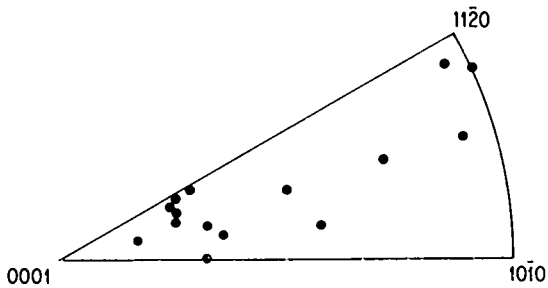

Fig. 2. Stereographic triangle showing the orientations of the whole set of available single crystals.

Table 1
Impurity analyses of Zr used in this work

	Zr I	Zr II	Zr III
Al	5	< 80	< 20
Ag	< 0.1	< 1	
Au	< 0.1		
B		< 2	< 0.05
Ca	0.2		< 50
Cd			< 0.2
Co		< 10	< 10
Cr	0.8	< 20	200
Cu	2.2	< 10	100–200
Fe	20	180	900
Ga	0.1		
Hf		< 200	
In	< 0.1		
K	1.5		
Mg	< 0.1	< 10	< 10
Mn		< 10	< 10
Mo	< 0.1	< 20	
Na	< 0.1		
Nb	< 0.1		
Ni	0.9	< 15	< 50
P	0.12		
Pb	< 0.1	< 10	< 20
Pd	< 0.1		
Pt	< 0.1		
S	1		
Sb	0.1	nd	
Si	5	< 50	100
Sn	2	< 10	< 400
Ti	< 0.1	< 30	< 20
V		< 10	< 50
W	< 0.1	< 100	< 50
Zn	0.86		

the orientations of the surface normal relative to the c axis of the set of single crystals from which diffusion samples for this study were chosen.

Single crystals were also obtained from two other less pure Zr rods. Impurity analyses of the three rods are shown in table 1.

2.2. Diffusion samples

Since large enough single crystals were available, it was decided to orient and cut them in such a way as to obtain, as far as possible, two samples from each one, with the diffusion direction (surface normal) parallel or perpendicular to the c axis. In the sample designation in table 2 the same arabic number refers to a common original single crystal, and the capital letter indicates different pieces of that crystal.

Mainly, two techniques were employed for surface preparation.

(a) In experiments 1, 2 and 4 (table 2) single crystals from the three kinds of Zr were mechanically polished in a specially designed rotating machine [10], which ensured sufficient flatness and parallelism of the surfaces. Subsequently these samples were electrolytically polished as was previously described.

(b) Another set of samples included in experiments 3, 5, 6 and 7 (table 2) were prepared using the spark-cutting technique. A Servomet apparatus, Model MD from Metals Research Ltd, with its accessories designed to shape single crystals, was used to cut and polish the samples. They were mounted in a two-circle goniometer, oriented by the Laue back-reflection X-ray method and cut. If necessary, they were again mounted and oriented and the selected surfaces were polished using the spark-cutting "planer". In this operation the tool was a brass disc of 20 cm diameter which rotates in a horizontal plane just above the samples. The area of the sample compared with the area of the disc is small enough to avoid border effects and a very flat surface (to within 5 μm in an area of 9×10^{-2} cm^2) can be obtained. The spark-polished samples were carefully cleaned with acetone and a short electrolytic polishing produced a mirror-like surface.

(c) One sample in experiment 5 underwent Ar-sputtering cleaning, which was performed after the sample had been mechanically polished. An Edwards High Vacuum Coating Unit, Model 12EG/1229 was used.

The sample geometry was not the same in all cases; it depended on the size and shape of the original crystal.

The samples were carefully cleaned before the tracer deposition. The radiotracer used was ^{51}Cr as $^{51}CrCl_3$ in 0.5M hydrochloric acid solution prepared by New England Nuclear Corp., USA. The specific activities of the solutions ranged from 217 kBq/kg to 421 kBq/kg. Using the technique described in ref. 14 the surface of the sample was electrolytically plated. The plating time varied from sample to sample according to the activity of the deposit per unit area planned for each one. Table 2 in §3 reports the specific activity per unit area of the deposit in each sample.

2.3. Diffusion experiments

The diffusion anneals were performed in an Ar atmosphere. At least two samples of different orientation were annealed together at each temperature. The experimental details for the diffusion anneals were described in ref. 12. The temperature was measured with a Pt–Pt 10% Rh thermocouple.

After the diffusion anneals, the samples were machined into cylinders. This procedure also served to eliminate the zone possibly affected by surface diffusion. The width of the zone eliminated was between $6\sqrt{Dt}$ to $9\sqrt{Dt}$. This operation was done in a precision lathe in which the ordinary tool was replaced by a portable dental lathe, supporting an abrasive disc. No damage on the diffusion surface could be detected by inspection with an optical microscope up to a magnification of 500×. The final diameters of the samples were between 0.25 cm and 1.0 cm.

Penetration profiles were determined by the direct sectioning method, following procedures described previously [12]. Layers were removed using an abrading machine [15]. In experiments 4 to 7 a Canberra 8100 Multi-Channel Analyzer was used in place of the single-channel spectrometer used before.

3. Results

The experimental set-up of the diffusion sample was planned to correspond to an "infinitely thin deposit of tracer on the flat surface of a semi-infinite specimen". In such a case the concentration $C(x, t)$ at a time t and a distance x from the surface is expressed by the Gaussian distribution

$$C(x,t) = \frac{S}{(\pi Dt)^{1/2}} \exp\left(-\frac{x^2}{4Dt}\right), \qquad (1)$$

where S is the total amount of tracer per unit area and D is the diffusion coefficient. Penetration profiles are straight lines when plotting log C versus x^2. D is obtained from the slope of these lines.

Gaussian profiles were obtained for all the samples

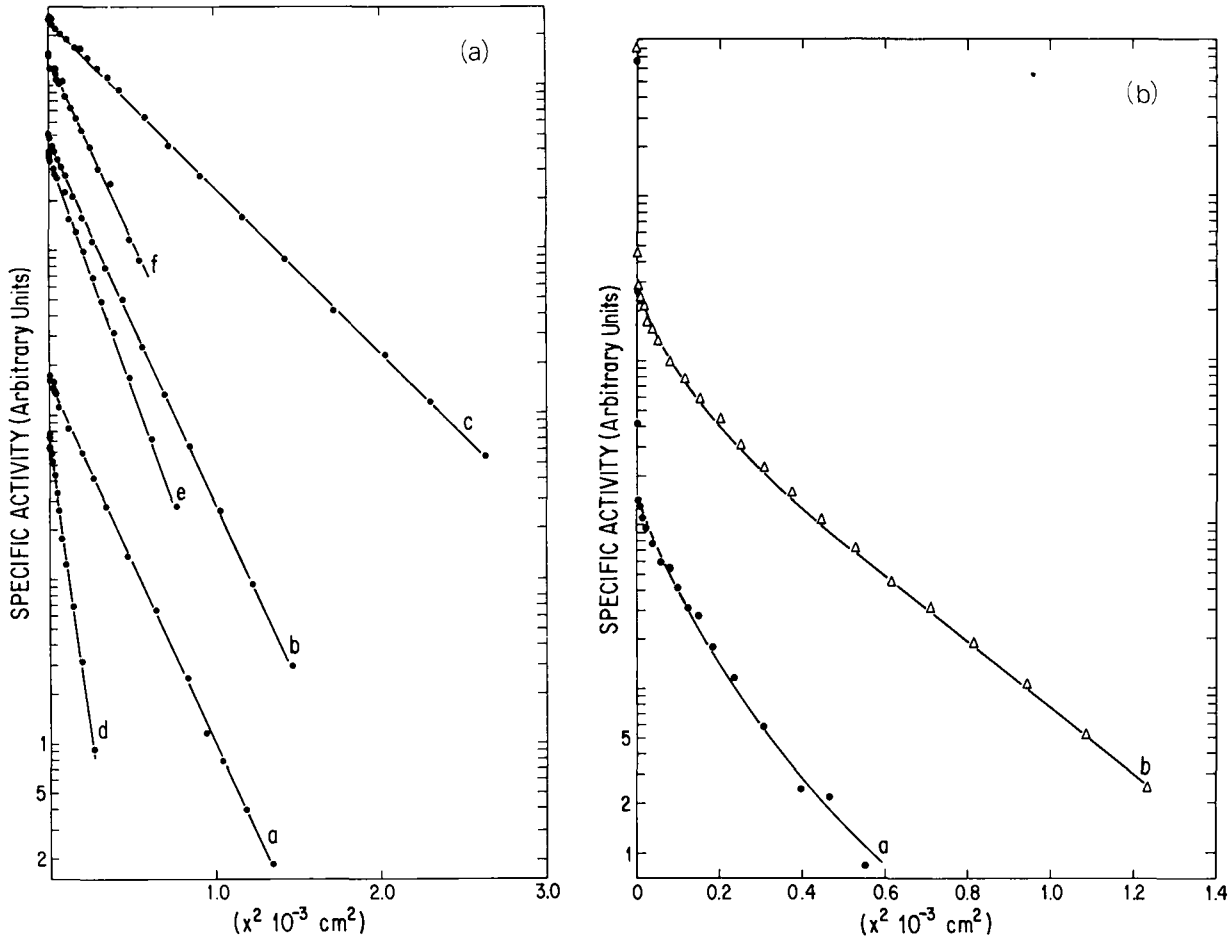

Fig. 3. (a) Typical Gaussian penetration profiles. a: 811°C 4.5 h, $\theta = 90°$; 848°C 2.5 h, b: $\theta = 88°$; c: $\theta = 31°$; 750°C 4 h, d: $\theta = 86°$, e: $\theta = 30°$; f: 789°C 3.58 h, $\theta = 30°$. (b) Typical non-Gaussian penetration profiles. a: 748°C 1 h, $\theta = 31°$; b: 816°C 7.25 h, $\theta = 86°$.

in experiments 3, 5, 6 and 7 and typical examples of these are shown in fig. 3a.

Table 2 summarises the characteristics and results of the whole series of experiments.

In experiments 1, 2 and 4, the penetration profiles of log C versus x^2 showed points of extremely high concentration very close to the surface (up to nearly 15 μm depth from the surface) and the rest of the plot with much lower concentration showed pronounced upward curvature. Fig. 3b shows typical examples of these profiles. This behaviour, which has also been found by other workers [3,16], is analyzed in the Appendix.

It is to be noted that all the plots for similar experiments show the same behaviour.

In experiments 3 and 5 for the two samples of the less pure Zr, D values smaller than the ones expected for their orientation were measured (fig. 7, Appendix). This could be ascribed to the dehancement of ^{51}Cr diffusion as a result of the larger impurity contents (e.g., Fe, Cu, Cr) (table 1) [3,17].

Only Gaussian profiles for Zr I samples (experiments 3, 5, 6 and 7) were used to perform calculations and to draw conclusions.

At each temperature, the coefficients for diffusion parallel ($D_{\parallel}$) and perpendicular ($D_{\perp}$) to the c axis were determined either directly ($\theta = 0°$ and 90°) or from measurements with two orientations of the surface normal (θ_1 and θ_2), by solving the equations:

$$D_{\theta_1} = D_{\perp} \sin^2\theta_1 + D_{\parallel} \cos^2\theta_1,$$

$$D_{\theta_2} = D_{\perp} \sin^2\theta_2 + D_{\parallel} \cos^2\theta_2. \qquad (2)$$

Table 2
Diffusion coefficients of ^{51}Cr in oriented α-Zr single crystals. $D_{\parallel}$ and $D_{\perp}$, characteristics of the diffusion experiments; S_t, surface treatment; M, mechanical polishing; SC, spark-cutting, planing; S, Ar sputtering, cleaning; A_s, activity of the deposit per unit area (counts/min cm^2)

T (°C)	t (h)	Exp.	Samples	θ (°)	S_t	$A_s \times 10^{-8}$	Penetration profiles	D_θ (10^{-13} m^2/s)	$D_{\parallel}$	$D_{\perp}$
590	120	1	Zr III 1 A	32	M	1.0	erfc	0.0266		
			Zr III 1 B	32		1.3		0.0262		
			Zr II 1 A	69		2.9		0.0281		
			Zr II 1 B	72		3.0		0.0374		
748	7	4	Zr I 3 C	31	M	3.5	erfc	1.38		
			Zr I 3 A	60		4.5		0.930		
750	4	6	Zr I 3 B	20	SC	0.22	Gaussian	2.45	2.64	
			Zr I 9 A	30		0.27		2.74	3.32	
			Zr I 9 B	86		0.19		1.03		1.03
789	3.58	7	Zr I 9 C	27	SC	0.27	Gaussian	4.17	4.85	
			Zr I 9 D	88		0.25		1.56		1.56
811	4.5	3	Zr I 2 A	0	SC	4.8	Gaussian	7.87	7.87	
			Zr III 1 A	30		1.3		3.14		
			Zr I 2 B	90		3.0		3.03		3.03
816	7.25	2	Zr III 1 A	34	M	2.0	erfc	1.95		
			Zr II 2	37		5.2		3.23		
			Zr I 2 B	86		7.1		2.06		
848	2.5	5	Zr I 6 A	31	SC	2.5	Gaussian	12.0	14.1	
			Zr I 3 C	32	M	3.0		11.6		
			Zr II 1 B	72	S	2.8		5.07		
			Zr I 6 B	88	SC	3.2		5.48		5.48

A least-squares fit of the diffusion data between 750°C and 848°C yielded the parameter values in the following expressions:

$$D_{\perp} = (0.2 \pm 0.2) \times 10^{-4} \times \exp\left(-\frac{(163 \pm 6)\text{kJ/mol}}{RT}\right)\text{m}^2/\text{s},$$

$$D_{\parallel} = (0.2 \pm 0.3) \times 10^{-4} \times \exp\left(-\frac{(153 \pm 11)\text{kJ/mol}}{RT}\right)\text{m}^2/\text{s}. \quad (3)$$

The corresponding Arrhenius plot is shown in fig. 4.

In this figure the size of the points represent the error in D, which was evaluated from the following analyses. Weights during sectioning were obtained with a precision of $\pm 10^{-5}$ g using a Mettler microscale, sample diameters were measured to within $\pm 5 \times 10^{-4}$

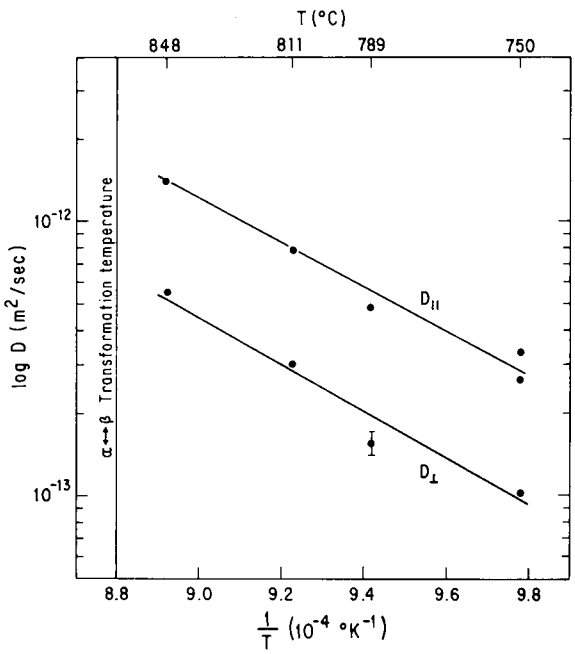

Fig. 4. Arrhenius lines for ^{51}Cr diffusion in α-Zr along the c axis and perpendicular to it. The error in D is represented by the size of the points except when specifically indicated.

Table 3
The anisotropy factor (f_a) for ^{51}Cr diffusion in α-Zr single crystals. Comparison with other solutes

Solutes	^{51}Cr	^{64}Cu [7]	^{58}Co [3]
$D_{\parallel}$ (m^2/s) 848°C	1.37×10^{-12}	4.76×10^{-12}	5.01×10^{-9}
848°C	2.7	3.0	8.3
f_a 750°C	2.9	3.2	5.2

cm and the activity of each layer was counted for long enough to ensure less than a 1% error. Under these conditions, error estimates done for each point in the penetration profile gave an error in D of less than 3%, except for $D_{\perp}$ at 789°C which was nearly 10%. In fig. 4 we have also to consider an uncertainty of ±2° in the determination of the angle and ±2°C in the annealing temperatures. The computer program used to obtain Q and D_0 values also calculates the errors in Q and D_0, taking into account the experimental error in the determination of D.

4. Discussion

Cr dissolves dissociatively in Zr and migrates interstitially. In α-Zr, Cr is a fast-diffusing solute, three orders of magnitude faster than self-diffusion [1].

Our measurements showed a significant anisotropy for Cr diffusion in the range of temperature studied, with $D_{\parallel} > D_{\perp}$ (fig. 4). The anisotropy factor $f_a = D_{\parallel}/D_{\perp}$ tends to increase as the temperature decreases. The same behaviour was seen in previous results for Cu diffusion in α-Zr [7], while the reverse is found for Co [3]. This is shown in table 3 where the diffusion coefficients were calculated with the corresponding Arrhenius equations [refs. 3, 7 and this work]. There it can also be seen that at a given temperature, the faster the solute the larger the anisotropy.

For the activation energies we obtained the result $Q_{\parallel} < Q_{\perp}$ (table 4). The same result for Au and Ag in Tl, another hcp metal, was interpreted by Anthony et al. [18] in terms of an interstitial diffusion mechanism within the framework of the hard-sphere model.

Table 4 contains $Q_{\parallel}$ and $Q_{\perp}$ for the three fast-diffusing solutes for which heterodiffusion in α-Zr single-crystals has been measured (refs. 3, 7, and this work). $Q_{\parallel}$ for Cr and Cu and $Q_{\perp}$ for Cr, Cu and Co at $T > 650$°C are comparable and the smaller the Q the larger the diffusion coefficient.

The ratio between the activation energy for solute- and self-diffusion was evaluated with heterodiffusion data in metallic solvents which admit fast-diffusing solutes [2,21], to perform a comparison with the corresponding value for Cr in α-Zr. Let $Q_{\parallel}$ or $Q_{\perp}$ for Cr and Cu or $Q_{\perp}$ for Co at $T > 650$°C be called Q_{solute} and consider for $Q_{self\text{-}diffusion}$ the value deduced when applying to α-Zr the semi-empirical rule $Q_{self\text{-}diffusion} = 35T_m$, with $T_m = 1870$ K [19,20]. Then $Q_{solute}/Q_{self\text{-}diffusion} = 0.5$–$0.6$, which falls in the range of 0.2–0.6 obtained for the fast metallic solutes diffusing in the high valency metals of groups III and IV [2,21]. However, if the measured value in α-Zr polycrystals for $Q_{self\text{-}diffusion}$ is adopted [10], $Q_{solute}/Q_{self\text{-}diffusion} \approx 1.3$. This value is close to that obtained for the dissociative solutes (Ni, Co, Fe and Cr among others) diffusing in Nb and in the bcc phases of Ti and Zr.

Comparison of the other diffusion parameter (the frequency factor D_0) shows very closely similar values [$(0.2$–$0.4)\times10^{-4}$ m^2/s] for Cr and Cu, while for Co there is an appreciable difference, up to 5 orders of magnitude.

It is interesting to compare Cr diffusion in both α and β phases of Zr. The activation energy is smaller in

Table 4
The activation energies for ^{51}Cr diffusion in α-Zr single crystals. Comparison with other solutes

		Increasing D_{solute} →			
		^{51}Cr	^{64}Cu [7]	^{58}Co [3]	
α-Zr	$Q_{\parallel}$ (kJ mol^{-1})	153	149	191	
	$Q_{\perp}$ (kJ mol^{-1})	163	154	146	($T > 650$°C)
				183	($T < 600$°C)
β-Zr	Q (kJ mol^{-1}) (914–1240°C)	143			

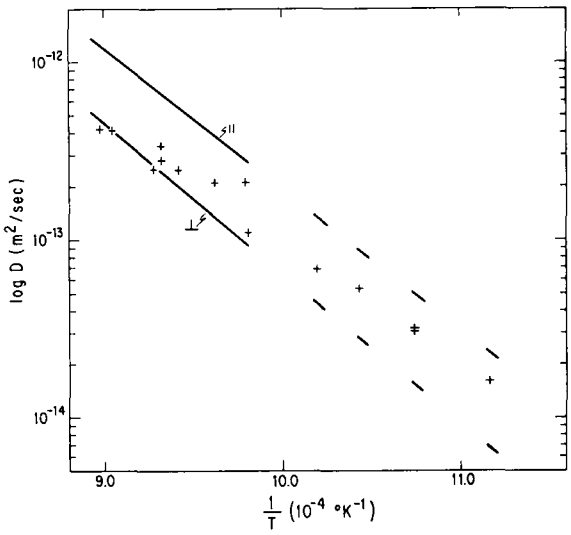

Fig. 5. ^{51}Cr diffusion coefficients in α-Zr polycrystals and the Arrhenius lines of this work. + polycrystals [8] [11]: ——— single crystals (this work).

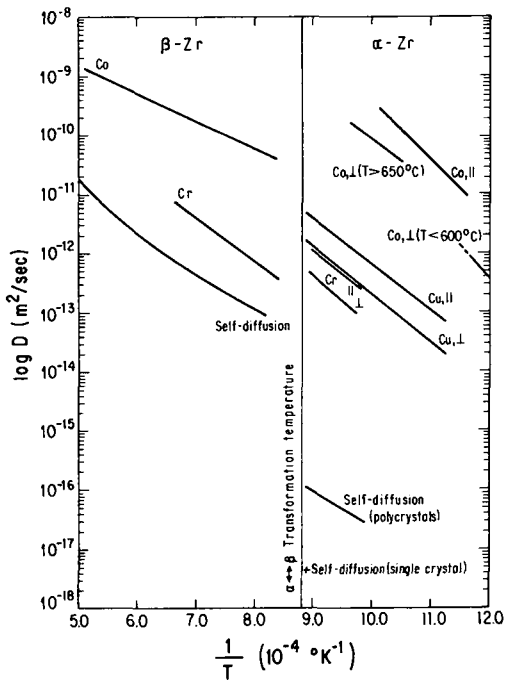

Fig. 6. Arrhenius plot for: Cr (this work), Cu [7] and Co [3] diffusion in α-Zr single crystals; Cr [11,22] and Co [24] diffusion in β-Zr; self-diffusion in both phases [10,25].

β-Zr [22] than in α-Zr, $Q_\beta < Q_{\alpha\parallel} < Q_{\alpha\perp}$, the difference being $Q_{\alpha\perp} - Q_\beta = 20$ kJ/mol. At the $\alpha \leftrightarrow \beta$ transformation temperature the Cr diffusion is slower in β-Zr than in α-Zr, but this change is small, showing thus only a slight sensitivity to the phase transition. The ratio of the diffusion coefficients in the two phases (D_β/D_α) is 0.29 for $D_{\alpha\parallel}$ and 0.11 for $D_{\alpha\perp}$. This behaviour compared with that of Zr self-diffusion – strongly sensitive to the transition and faster in the β-phase (the ratio here is 300) – was interpreted in terms of the hard-sphere model and appears as a characteristic of the interstitial diffusion of most dissociative solutes [10,18,23].

Fig. 5 shows the previous measurements of Cr diffusion coefficients in α-Zr polycrystals [8,11,12] and the Arrhenius lines obtained in this work. As was supposed, the measurements in polycrystals are contained between the Arrhenius straight lines for $D_\parallel$ and $D_\perp$ and their extrapolations to temperatures lower than 750°C. This confirms the influence of the anisotropy on the different measurements in polycrystals through the differing orientation of the various grains forming each sample.

Finally, on fig. 6 are shown the Arrhenius graphs for diffusion of Cr, Cu and Co in single crystals of α-Zr (refs. 7, 3 and this work) compared with the diffusion of Cr and Co in β-Zr [22,24] and with self-diffusion in both phases [5,10,25].

Appendix. Non-Gaussian profiles

The first points of high activity in the profiles of experiments 1, 2 and 4 could be an indication of the hold-up of the radiotracer in the surface during the course of annealing.

These experiments, compared with experiment 3, suggested that the hold-up might be a consequence of the surface treatment of the sample before the tracer deposition. In experiment 5 three different types of surface treatments were used in different samples (table 2) obtaining Gaussian profiles for all of them. So, no influence of the surface treatment was proved at least at high temperatures.

The very low solubility of Cr in α-Zr [26] may be another source of tracer hold-up owing to the incomplete dissolution of the deposit during the annealing time. So, the amount of the deposits in experiments 6 and 7 was reduced by approximately one order of magnitude, obtaining Gaussian profiles (table 2). The comparison of these experiments with 1 and 4 provides evidence of the influence of solubility when abundant deposits are used.

Finally an attempt to fit the penetration profiles of

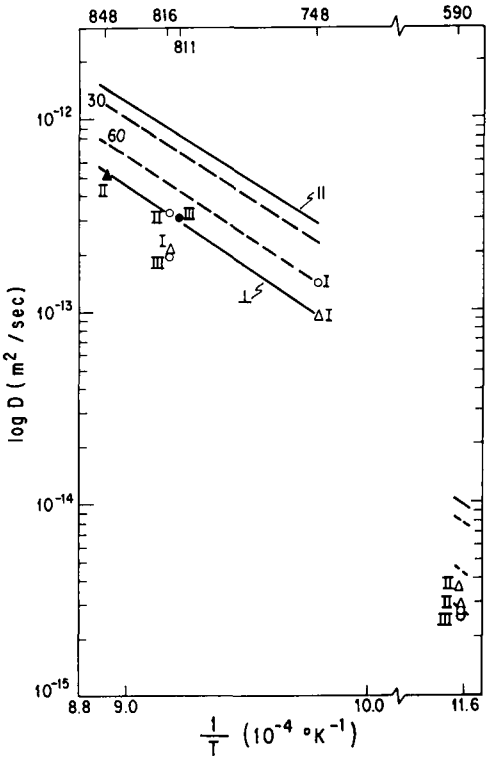

Fig. 7. D_θ measured in the less pure Zr samples. D_θ obtained from non-Gaussian penetration profiles and the Arrhenius lines of this work. D_θ: $\bigcirc \approx 30°$, $\triangle \geq 60°$; open circles or triangles represent a non-Gaussian profile (erfc) and filled circles or triangles represent a Gaussian profile; I, II, III denote Zr purity. Arrhenius lines (this work): ——— $\parallel c$ and $\perp c$; — — — $\theta = 30°$ and 60° [calculated from eqs. (3) and (2)].

experiments 1, 2 and 4 with the solution of the diffusion equation for "constant surface concentration (C_0)"

$$\frac{C(x,t)}{C_0} = \operatorname{erfc}\left(x/2\sqrt{Dt}\right) \qquad (4)$$

gave the results shown in table 2. These figures are lower than the ones calculated (for the same orientation and temperature) using one of the two parts of eq. (2) where $D_\parallel$ and $D_\perp$ are obtained from eq. (3). This is clearly shown in fig. 7 where the Arrhenius lines of fig. 4 are drawn together with these values. Thus eq. (4) seems not to be an appropriate solution for these cases.

Acknowledgements

The authors are grateful to Dr A.D. Le Claire for suggesting the idea behind this study and for stimulating discussions during its development, to Lic.L.I. Nicolai for her collaboration in obtaining the single crystals and during the first experiments and to Dr R. Migoni for a critical reading of the manuscript. This work was partially financed by the Comisión de Investigaciones Científicas de la Provincia de Buenos Aires, Argentina.

References

[1] R. Tendler, E. Santos, J. Abriata and C.F. Varotto, in: Thermodynamics of Nuclear Materials 1974, Vol. II (IAEA, Vienna, 1975) p. 71.
[2] W.K. Warburton and D. Turnbull, in: Diffusion in Solids, eds., A.S. Nowick and J.J. Burton (Academic Press, New York, 1975) p. 171.
[3] G.V. Kidson, Phil. Mag. A44 (1981) 341.
[4] G.M. Hood and R.J. Schultz, Phil. Mag. 26 (1972) 329.
[5] G.M. Hood and R.J. Schultz, Acta Met. 22 (1974) 459.
[6] R. Tendler, J. Abriata and C.F. Varotto, J. Nucl. Mater. 59 (1976) 215.
[7] G.M. Hood and R.J. Schultz, Phys. Rev. B11 (1975) 3780.
[8] R. Tendler and C.F. Varotto, J. Nucl. Mater. 44 (1972) 99.
[9] R. Tendler and C.F. Varotto, J. Nucl. Mater. 46 (1973) 107.
[10] F. Dyment and C.M. Libanati, J. Mater. Sci. 3 (1968) 349.
[11] L.I. Nicolai, R. Migoni and R.H. de Tendler, J. Nucl. Mater. 115 (1983) 39.
[12] L.I. Nicolai and R.H. de Tendler, J. Nucl. Mater. 82 (1979) 439.
[13] N. Varela, L.I. Nicolai, S.N. Balart and R.H. de Tendler, CNEA-NT 1/81 (1981).
[14] E. Santos and F. Dyment, Plating 60 (1973) 821.
[15] Y. Adda and J. Philibert, La Diffusion dans les Solides, Vol. I (Presses Universitaires de France, Paris, 1966) p. 256.
[16] G.M. Hood, in: Diffusion Processes, eds., J.N. Sherwood, A.V. Chadwick, W.M. Muir and F.L. Swinton (Gordon and Breach, London, 1970) p. 361.
[17] D.L. Decker, J.G. Melville and H.B. Vanfleet, Phys. Rev. B20 (1979) 3036.
[18] T.R. Anthony, B.F. Dyson and D. Turnbull, J. Appl. Phys. 39 (1968) 1391.
[19] A.D. Le Claire, in: Diffusion in Body-Centered Cubic Metals (Am. Soc. Met., Metals Park, Ohio, 1965) p. 3.
[20] A.J. Ardell, Acta Met. 11 (1963) 591.
[21] A.D. Le Claire, J. Nucl. Mater. 69/70 (1978) 70.
[22] L.I. Nicolai and R.H. de Tendler, J. Nucl. Mater. 87 (1979) 401.
[23] M.P. Dariel, in: Handbook on the Physics and Chemistry of Rare Earths, eds., K.A. Gschneider Jr. and L. Eyring (North-Holland, Amsterdam, 1978) p. 847.
[24] G.V. Kidson and G.J. Young, Phil. Mag. 20 (1969) 1047.
[25] J.I. Federer and T.S. Lundy, Trans. Met. Soc. AIME 227 (1963) 592.
[26] M. Hansen, Constitution of Binary Alloys (McGraw-Hill, New York, 1958); F.A. Shunk, Second Supplement, Constitution of Binary Alloys (McGraw-Hill, New York, 1966).